

This poster builds upon the earlier work of Osborn *et al.* (1999), Ulbrich *et al.* (1999), Zorita & Gonzalez-Ruiz (2000), Osborn (2004) and others, in evaluating and applying climate model simulations to answer a number of questions about the North Atlantic Oscillation. This study expands the comparison to include many different global climate models, using simulations undertaken for the IPCC 4th assessment report. The pre-industrial control runs, the 20th century forced runs and the future simulations under the SRES A1B scenario are used here. Throughout this work, seasonal-mean winter (December to March) sea level pressure (SLP) data are used, and the North Atlantic Oscillation and its index are defined as the leading empirical orthogonal function (EOF) and associated principal component (PC) time series of the Atlantic half of the Northern Hemisphere SLP field.

The **first column** (hPa) of maps shows how well the models reproduce the winter SLP climatology (see also the pattern correlation values at the right-hand side). The large scale features are reasonably simulated, though their absolute values are sometimes in error. The leading mode of Atlantic-sector inter-

annual variability (**column two**, expanded to give hemispheric patterns), defined by the leading EOF of SLP from each model's control run, is clearly the NAO in all cases. Projecting observed SLP onto the simulated EOFs results in time series that closely match the observed leading PC, indicating that biases in the simulated NAO patterns are relatively unimportant. Nevertheless, they are interesting, with the main bias being a tendency for enhanced correlation with the North Pacific SLP in some models (becoming closer to an Arctic Oscillation, despite being defined using only Atlantic-sector SLP). In most models, this leading EOF explains more variance than is the case for the observations.

If we keep this definition of the NAO constant, and then project the SLP from simulations with increasing greenhouse gas concentrations (SRES A1B simulations) onto the control run EOFs, we yield the time series shown below. Most models indicate increasing values of the NAO index, though with varying magnitude. The reason for these trends is that there is a long-term trend in the SLP patterns in most models when enhanced greenhouse forcing is applied (**column three**, hPa per century),

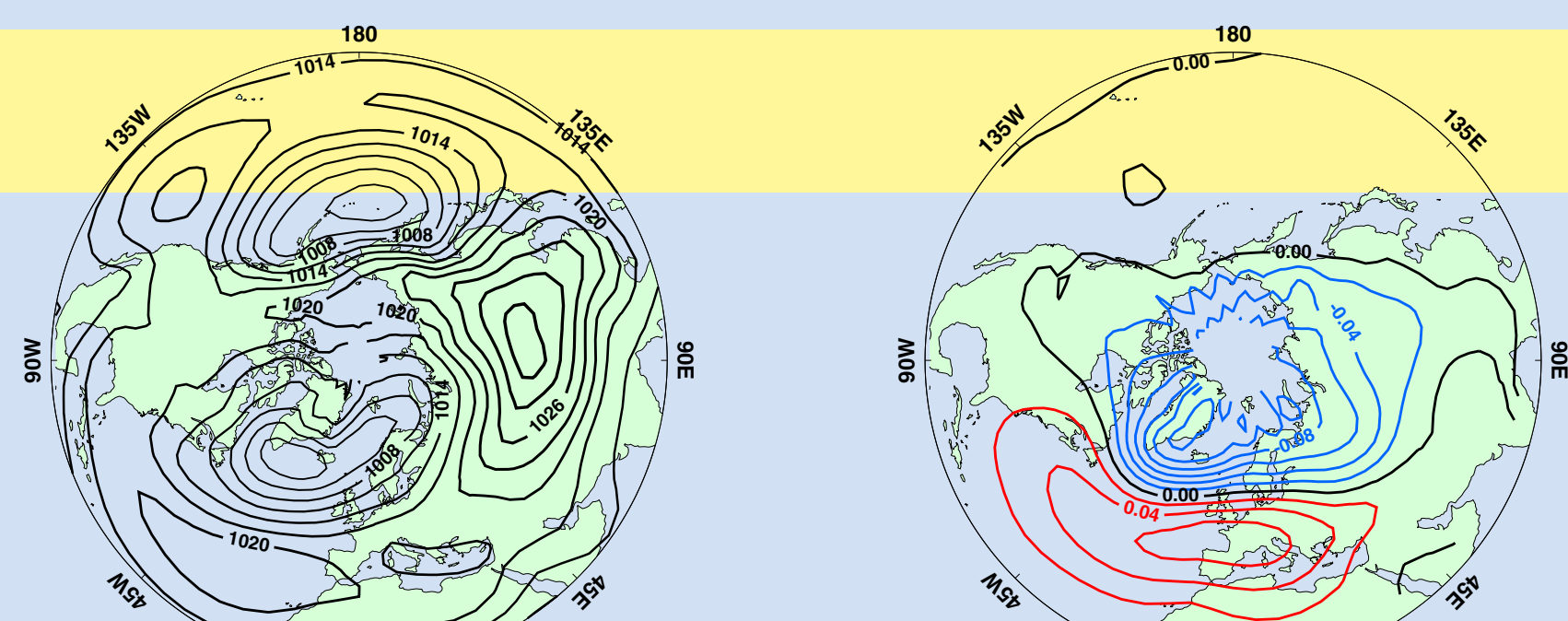
which either resembles the NAO or at least has some power over the NAO centres of action.

An alternative approach is to allow the NAO definition to alter and diagnose how the oscillation itself may change under enhanced greenhouse forcing. The **fourth column** indicates the EOFs of the (detrended) SLP field computed from the 2050-2099 period of the SRES A1B simulations. Under the altered forcing, the NAO explains a similar - or perhaps slightly more - amount of variance (when considering all models together), though the interannual variability may be lower. The EOF patterns show a number of changes: in some, the Azores centre of action shifts eastward (and slightly northward), while in some the Iceland centre of action shifts eastward; some models simulated an intensification of the Azores centre of action, while others show the reverse.

Further work is in progress, assessing temporal variability changes and comparing recent observed NAO changes with the range of variability simulated by the climate models (see, e.g., Osborn, 2004).

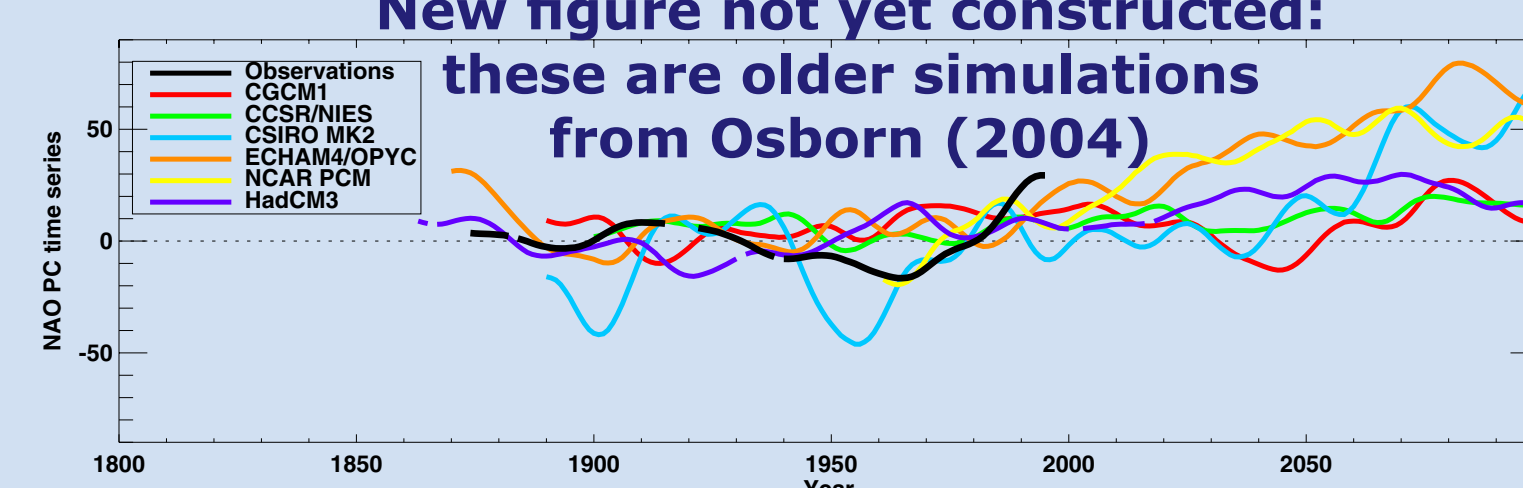
## Observations

UKMO sea level pressure analyses 1873-1995 (Jones, 1987; Basnett & Parker, 1997)



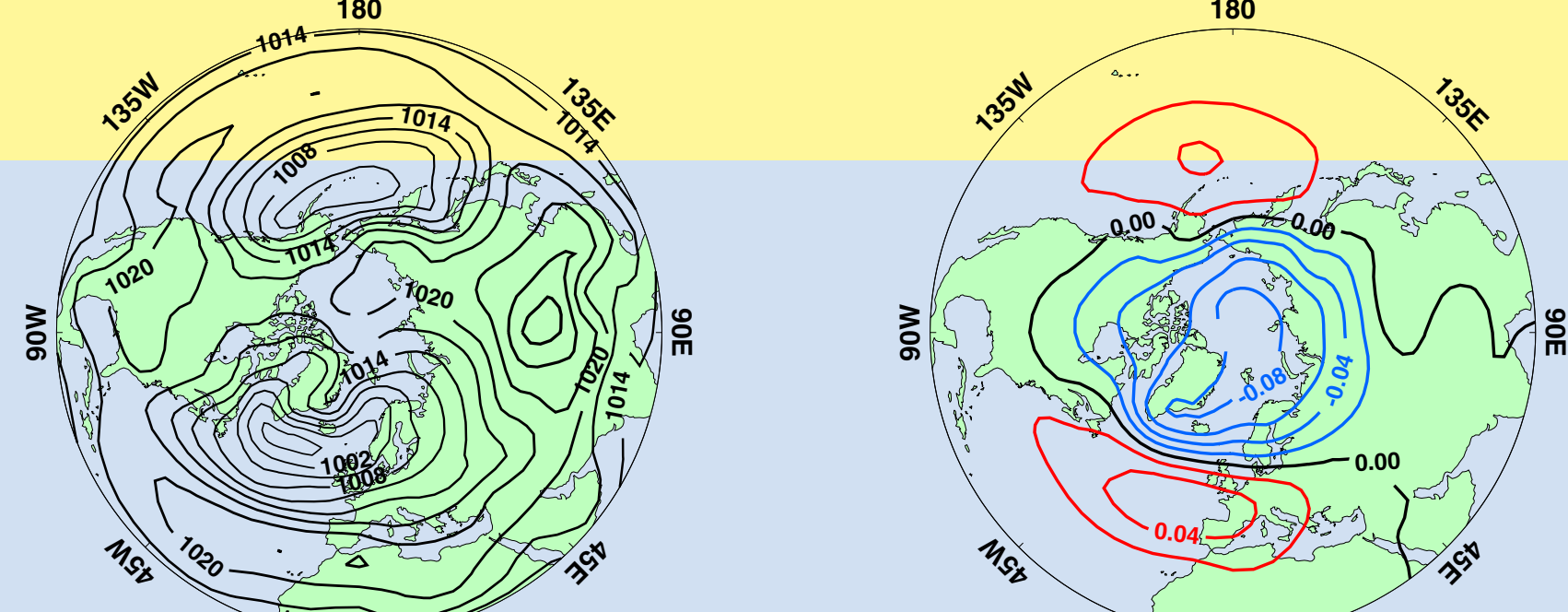
### New figure not yet constructed:

these are older simulations from Osborn (2004)



Smoothed time series showing the NAO indices from the greenhouse gas forced simulations, when their SLP fields are projected onto the corresponding control run NAO patterns. Observed NAO time series is also shown.

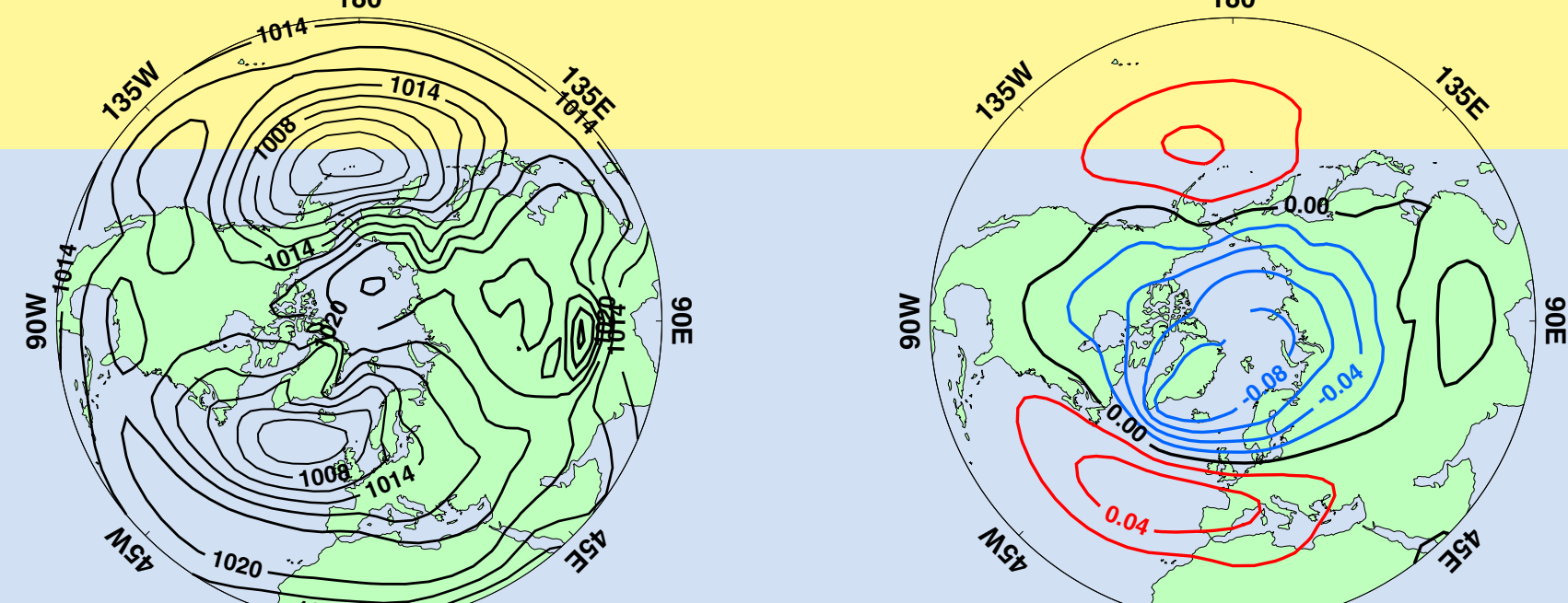
## CNRM\_CM3



## CNRM\_CM3

**pattern:** 0.89  
**% con:** 53  
**% a1b:** 56

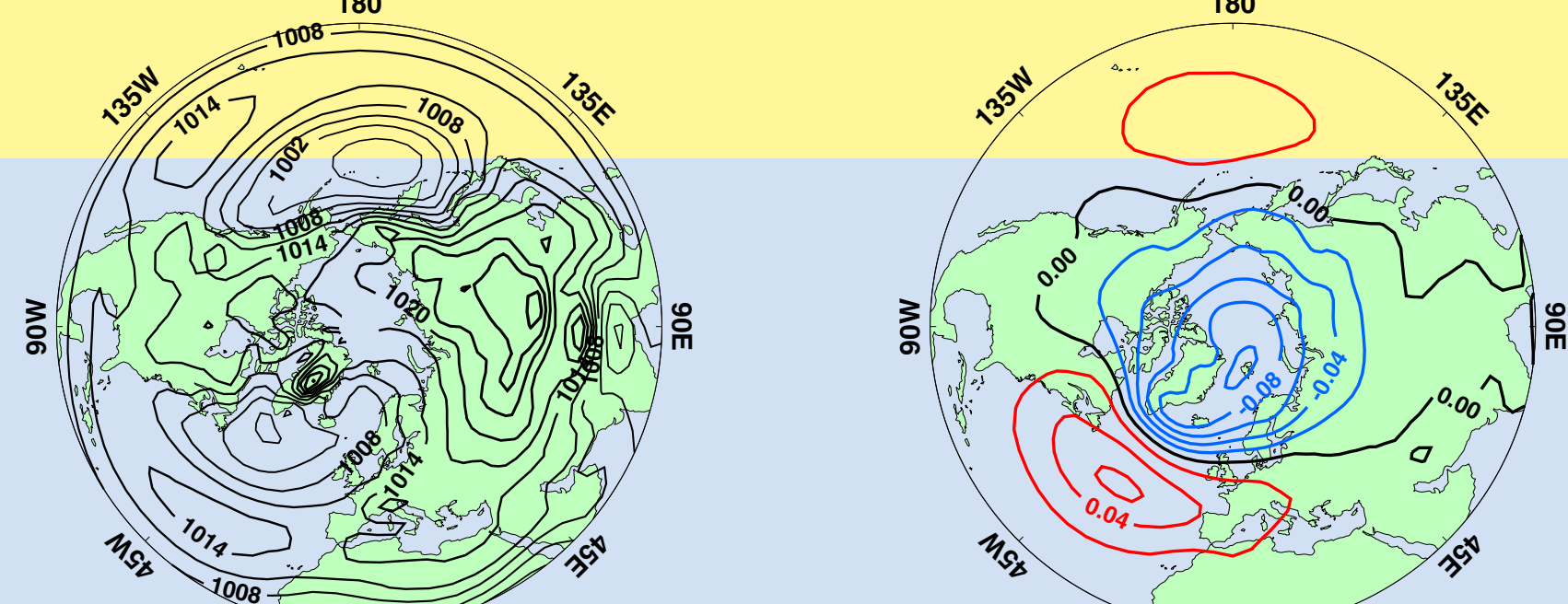
## GFDL\_CM2\_0



## GFDL\_CM2\_0

**pattern:** 0.86  
**% con:** 56  
**% a1b:** 64

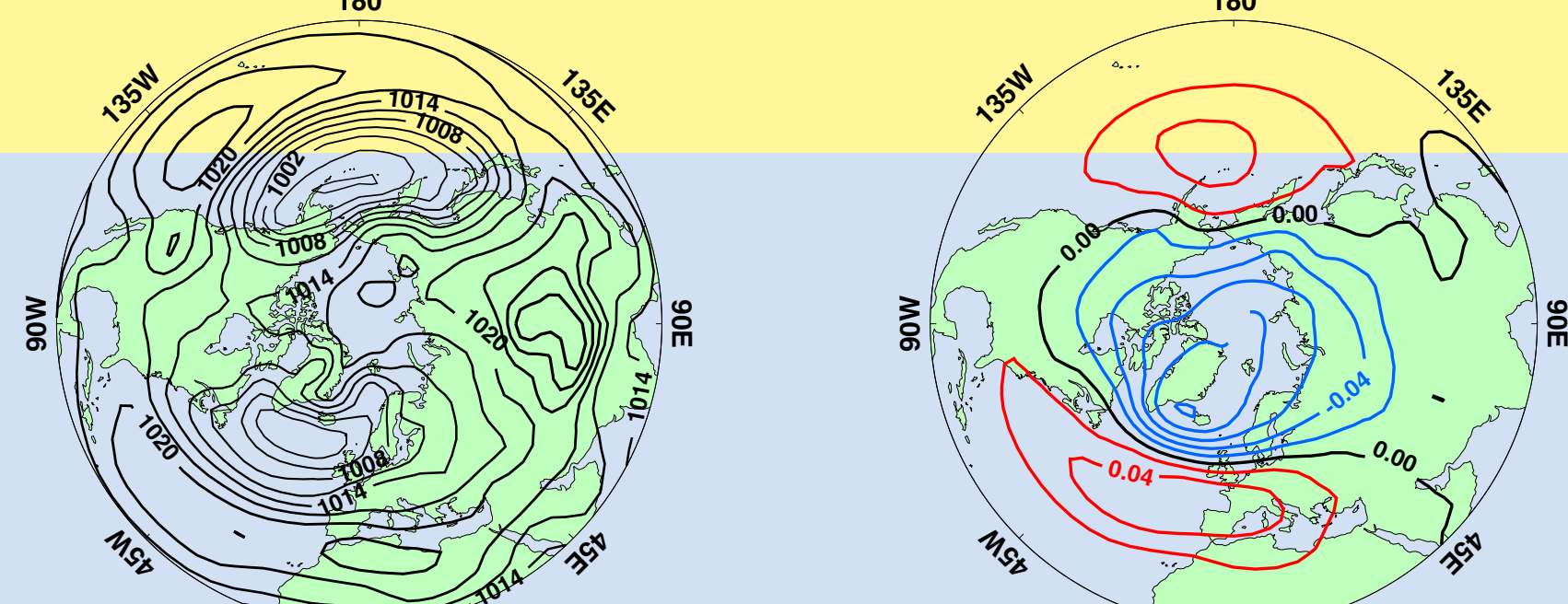
## GISS\_MODEL\_E\_H



## GISS\_MODEL\_E\_H

**pattern:** 0.81  
**% con:** 51  
**% a1b:** 53

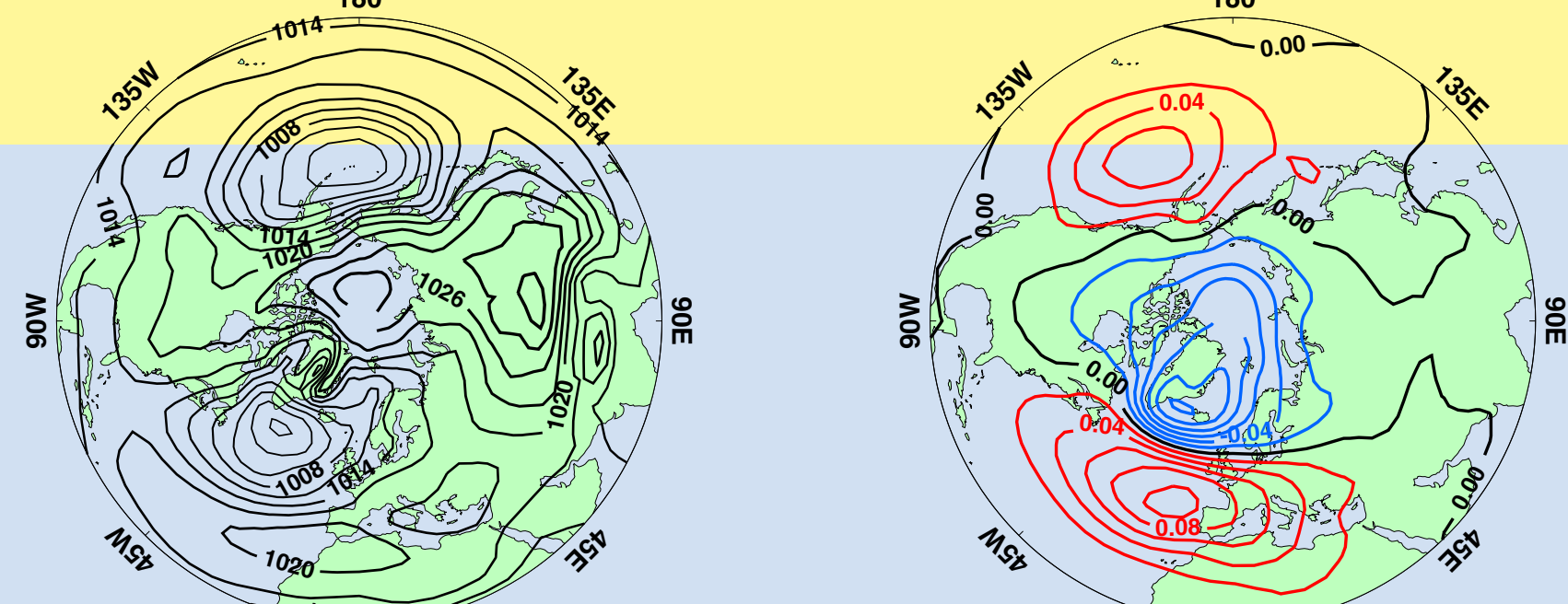
## MIROC3\_2\_medres



## MIROC3\_2\_medres

**pattern:** 0.82  
**% con:** 53  
**% a1b:** 53

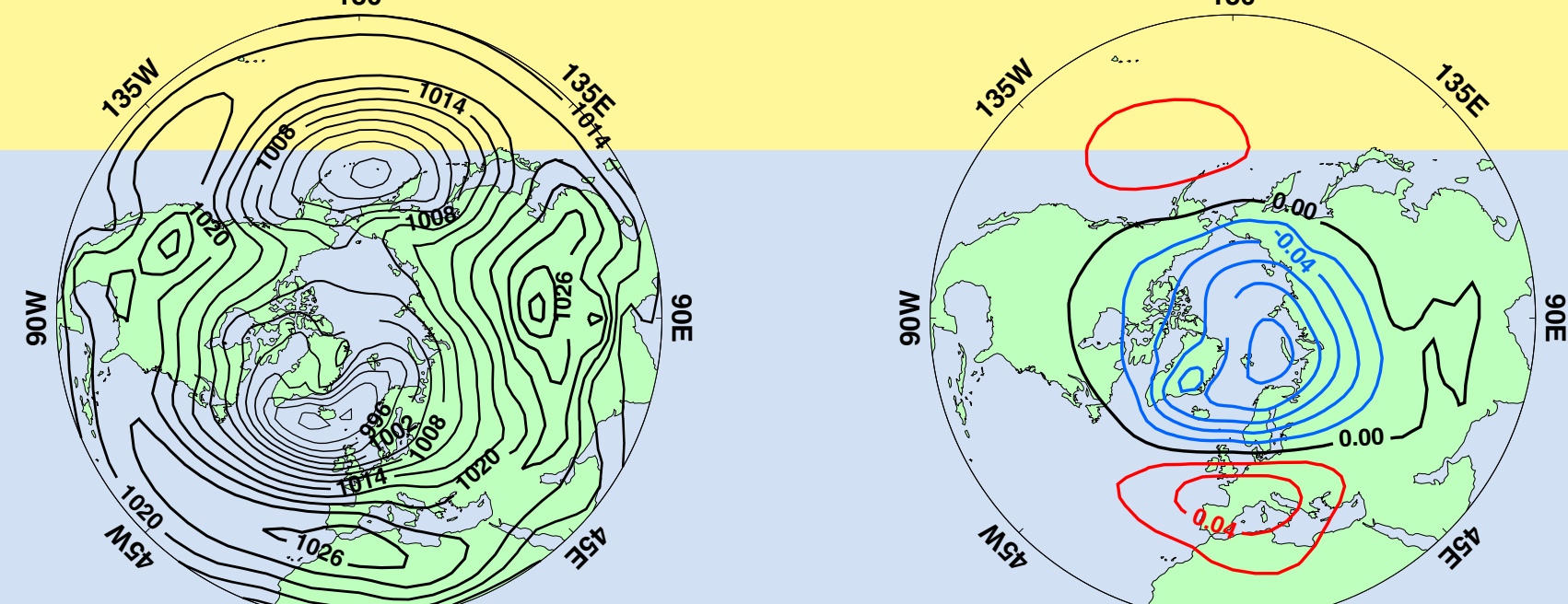
## MRI\_CGCM2\_3\_2a



## MRI\_CGCM2\_3\_2a

**pattern:** 0.84  
**% con:** 57  
**% a1b:** 56

## NCAR\_CCSM3\_0



## NCAR\_CCSM3\_0

**pattern:** 0.79  
**% con:** 57  
**% a1b:** 56

This column is computed from trends over the slightly different periods in each model, which may explain some of the inter-model differences